Phase structure development as preheating UHMWPE powder temperature changes in the micro-UPM process

2016 J. Micromech. Microeng. 26 015014

(http://iopscience.iop.org/0960-1317/26/1/015014)

IOP Publishing Journal of Micromechanics and Microengineering

J. Micromech. Microeng. **26** (2016) 015014 (9pp) doi:10.1088/0960-1317/26/1/015014

Phase structure development as preheating UHMWPE powder temperature changes in the micro-UPM process

Xiong Liang[1,2], Xiaoyu Wu[1], Bin Xu[2], Jiang Ma[2], Zhiyuan Liu[2], Taijiang Peng[1] and Lianyu Fu[3]

[1] Shenzhen Key Laboratory of Advanced Manufacturing Technology for Mould & Die, Shenzhen University, Shenzhen 518060, People's Republic of China
[2] College of Mechatronics and Control Engineering, Shenzhen University, Shenzhen 518060, People's Republic of China
[3] Shenzhen Jinzhou Precision Technology Corp., Shenzhen 518116, People's Republic of China

E-mail: wuxy@szu.edu.cn and xubin_szu@163.com

Received 20 January 2015, revised 10 November 2015
Accepted for publication 18 November 2015
Published 15 December 2015

Abstract

In this study, using high-speed mechanical drilling on printed circuit boards (PCBs) with two micro carbide drill bits with diameters of 0.15 mm and 0.20 mm, two different PCB micro-cylinder array inserts are fabricated using the micro-ultrasonic powder moulding (micro-UPM) process. According to the temperature curves recorded by a measurement module, when viscoelastic heating dominated, the temperature increasing rate was about three times the rate when interfacial friction heating dominated. From the differential scanning calorimetry and nanoindentation test results, if the ultra-high molecule weight polyethylene (UHMWPE) powder was not preheated, then the micro-cylinder array polymer parts generally consisted of nascent and melt-recrystallised phases as a whole. However, when the micro-cavity and compressed UHMWPE powder grew from room temperature of 28 °C to 85 °C, the two-phase structure gradually developed into a single melt-recrystallised phase. According to single-crystal x-ray diffraction test results, the crystallinity of the base region of the micro-UPM cylinder array part is higher than that of the micro-cylinder region, whereas the grain size of the (1 1 0) crystal surface is larger than that of the (2 0 0) crystal surface.

Keywords: compression moulding, ultrasonic vibration, ultra-high molecular weight polyethylene, micro-cylinder array

(Some figures may appear in colour only in the online journal)

1. Introduction

Micro-array parts, such as the nozzle plates of high-speed printers, optical fibre connectors, micro filters, the gratings of electron microscopes, biological micro-needle arrays, optical memories, and micro-chemical reaction chips, are widely used at present in medical facilities, communication, optics, and chemistry. For micro-array fabrication, the techniques commonly used are photolithography, ion etching, synchrotron x-ray lithography, excimer laser processing, hot embossing, and micro-injection moulding, to name a few [1, 2]. Research on micro-array structure mould inserts has also been widely conducted. Takahata *et al* succeeded in fabricating a microelectrode array with a diameter of 20 μm and a pitch of 60 μm using a lithography process. Utilising this microelectrode array, they fabricated a micro-hole array with a diameter of 30 μm on a stainless steel sheet using the micro-electron discharge machining (micro-EDM) process [3]. Applying the micro-electrochemical machining (micro-ECM) process, Kurita *et al* fabricated a prismatic micro-electrode

with a side length of 200 μm by using nickel particles with a diameter of 500 μm as the raw material. With this electrode, they fabricated a micro-square hole on a 200 μm-thick nickel plate [4]. Using inductively coupled plasma (ICP) on silicon-based mould inserts, Lu *et al* fabricated four 10 $\times$ 10 micro-hole array inserts with diameters of 60, 90, 110, and 130 μm and a depth of 250 μm [5]. Cherng *et al* presented a novel method fabricating microlenses on polydimethylsiloxane (PDMS) by the thermal reflow technique, followed by multiple replication processes to transfer the microlenses from the planar substrate onto a spherical surface, the curvature radius of which was approximately 6.1 mm [6]. Liu *et al* fabricated a PDMS membrane with microlens arrays using soft photolithography techniques and air-assisted negative pressure. The PDMS membrane was then used as a mould insert to achieve polycarbonate micro-lens array parts by the hot embossing technique [7]. All of the researchers mentioned above have explored the fabrication of micro-array inserts well.

Fu *et al* designed and fabricated a micro-drill bit with a high aspect ratio and proposed a method to fabricate micro-holes with a high depth-to-diameter ratio on printed circuit boards (PCBs). They also analysed how the key parameters of micro-drill bits affect the quality of PCB hole-wall roughness [8, 9]. Based on the research of Fu *et al*, Liang *et al* successfully fabricated three types of micro-hole array PCB insert, and produced three micro-cylinder array parts by the micro-ultrasonic powder moulding (micro-UPM) process; the size effects on the three PCB inserts during the moulding process were also investigated [10]. From the experiment conducted above, the use of a high-speed mechanical drill guarantees micro-holes with a high aspect ratio, and micro-UPM is proven to have some advantages, such as low cost, high production efficiency, and good consistency.

Ma *et al* fabricated three types of metallic glass micro-moulds with irregular array channels to study the moulding-filling kinetics of viscous metallic glass in its super-cooled liquid state [11]. Ma *et al* successfully fabricated micro-hole and micro-grating arrays, due to the unique thermoplastic forming ability of the model Pd-base metallic glass in the super-cooled liquid region. Subsequently, they reproduced two different structures of micro-arrays on four typical thermoplastic polymers by a hot embossing process [12]. Zhang *et al* fabricated micro-cavity inserts of Pd-base metallic glass $Pd_{40}Cu_{30}Ni_{10}P_{20}$ with a micro-square array and micro-cylinder array; using micro-hot embossing and micro-injection moulding, they successfully reproduced two different structures of micro-arrays on three typical thermoplastic polymers [13].

In the micro-UPM process, the powder (including polymer and eutectic alloy powder) prefilled and compacted in the barrel is rapidly heated and plasticised with ultrasonic vibration. Next, the entire micro-cavity is filled under compression pressure (the working end surface of the sonotrode reaches above 16.0 MPa), and the micro-parts are moulded. In the ultrasonic assisted plasticisation moulding study, Fairbanks experimented with thermoplastic and thermosetting plastic powder with an output frequency of 20 kHz low-power ultrasound. Without external heat in this experiment, the thermoplastic powder was successfully melted merely by ultrasonic frictional heat and sonotrode pressure [14]. Paul *et al* practised polypropylene (PP) powder compression moulding with ultrasonic welding equipment whose power is 900 W and output frequency is 20 kHz, through which they optimised the tensile strength of the plastic parts [15].

The preceding studies all focused on macroscale moulding. However, to obtain well-plasticised melts and acceptable parts by ultrasonic compression moulding, the power of the ultrasound plasticisation equipment mentioned above is less likely to obtain well-plasticised melts and acceptable plastic parts. To address this problem, Michaeli *et al* developed a micro-ultrasonic direct injection moulding system. Under the compound effects of ultrasonic vibration and sonotrode pressure, melted PP flowed into the mould cavity through micro-channels and a 1:16 micro-tensile bar, a micro-gear, and a thin cover plate with three holes fabricated [16]. Using polylactide (PLA) powder, Matias *et al* developed an ultrasonic micro-moulding system to fabricate small-sized samples (tensile and guitar samples). With the optimisation of the ultrasonic amplitude and moulding pressure, degradation was prevented, and both structural features and mechanical properties were preserved [17]. In the process of nanocomposites from PLA, polybutylene succinate (PBS), and four natural and organo-modified montmorillonite powders by Marc *et al* ultrasonic energy renders exfoliated nano-montmorillonite powder with high orientation in the direction of the polymer flow, as evident in transmission electron micrograph (TEM) and x-ray diffraction (XRD) data [18]. Wu *et al* fabricated three types of micro-gears with a micro-ultrasonic moulding process using Sn-Bi eutectic alloy powder as the raw material. They also investigated the effect of ultrasonic exposure time on the microstructure and mechanical properties of micro plastic parts [19]. Zeng *et al* used non-preheated iPP powder as the raw material for the research of micro-UPM and the thermal property and tensile mechanical properties of micro plastic parts [20]. Using ultra-high molecule weight polyethylene (UHMWPE) powder as the raw material, Liang *et al* successfully fabricated micro gears by micro-UPM. In addition, they investigated the morphology evolution using scanning electron microscopy (SEM) at different ultrasonic times, the two-phase structure and moulding mechanism using differential scanning calorimetry (DSC) and nanoindentation tests, as well as the compressive mechanical properties using a universal material tester [21].

Unlike previous studies [10, 20, 21], a brand new approach is introduced in this paper. First, UHMWPE powder with an average particle size of 150 μm was directly filled into the micro-cavity with a micro-hole PCB array insert. Second, the powder was repeatedly compressed using an ultrasonic sonotrode. Third, a heating device was used to preheat the entire micro-combined mould with powder prefilled. After the proper process parameters on the micro-UPM experimental platform had been set, micro-cylinder array polymer parts were successfully moulded. According to the temperature curves recorded by a measurement module, when viscoelastic heating dominated, the temperature increasing rate was about three times the rate when interfacial friction heating effect dominated. The densities of the raw material powder, the billet (compacted powder) and the micro-UPM parts were measured

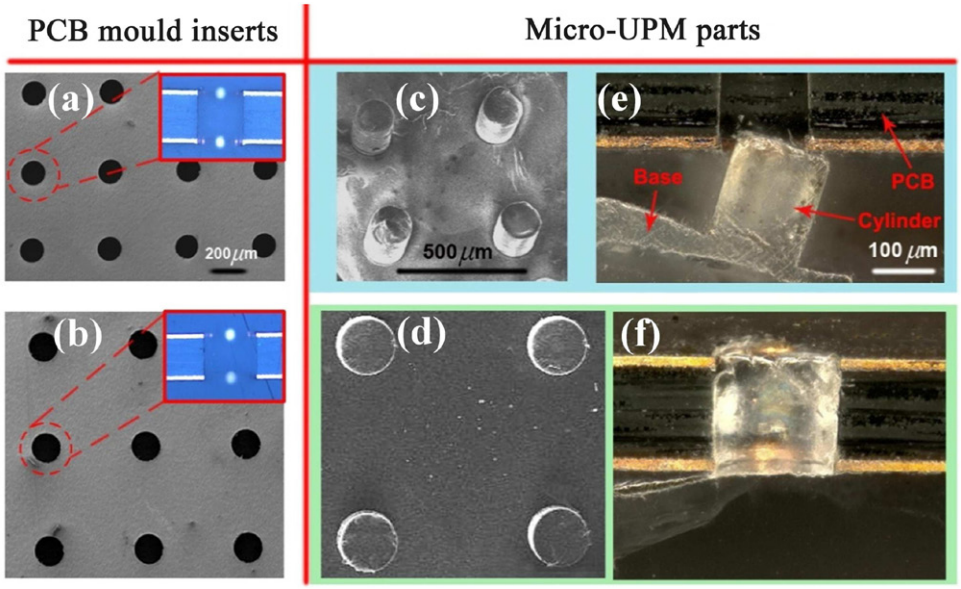

Figure 1. PCB micro-inserts and micro-UPM polymer parts: (a), (c) and (e) are the micro-inserts of diameter 0.15 mm; (b), (d) and (f) are the micro-inserts of diameter 0.20 mm. The red circles indicate the selected micro-hole slices.

at different powder preheated temperatures. According to the DSC, nanoindentation and single-crystal XRD test results, the phase structure development of micro-UPM UHMWPE polymer parts as a function of powder preheated temperature was investigated.

2. Experiment

The diameters of the micro-carbide drill bits are 0.15 mm and 0.20 mm. The thickness of PCB after copper deposition is approximately 185.0 μm. The PCB micro-cavity insert with micro-hole arrays is fabricated via high-speed mechanical drilling on a CNC drilling machine (NC-GN1210E, Hitachi). On two types of PCB micro-cavity inserts, we randomly select 20 holes (10 for each type) and measure their diameters and depths using a surface profiler (WYKO NT9300, VEECO), with the mean values of 164.5 μm and 211.6 μm and the standard deviations of 2.6 and 2.1, respectively. The depths of the two types of micro-holes are 182.5 μm and 182.5 μm, with standard deviations of 2.9 and 1.9, respectively. To measure the roughness of the micro-hole wall, we conduct cold inlaid separately on these two PCB micro-cavity inserts and polish them to the maximum diameter of micro holes. The average values of roughness of the two types of inserts measured are 3.6 μm and 3.3 μm, respectively, with standard deviations of 0.3.

The micro-UPM experimental platform is a modification of the RS2026 ultrasonic plastic welder produced by the Shenzhen Hongri Ultrasonic Equipment Cooperation. The equipment power is 2600 W and the output frequency of the ultrasonic horn is 20 kHz. The diameters of the piston in the welder cylinder and the working end surface of the sonotrode are 63 mm and 5 mm, respectively. Therefore, the air pressure is amplified by approximately 160 times upon transmission to the ultrasonic sonotrode. That is, when the pressure in the air cylinder is 0.1 MPa, the compression pressure of the working end surface of the sonotrode reaches approximately 16.0 MPa.

The heating device consists of a silica gel heating plate and a temperature control instrument. The thickness of the silica gel heating plate is 1.8 mm, the heating power density is 1.2 W·cm^{-2} and mechanical pressure resistance is 100 kg·cm^{-2}. The temperature control instrument (Model: CHB702-011-01111013) measures temperature from −50 °C to 1600 °C with an error of ±0.5 °C and working voltage 220 V.

A detailed introduction of the micro-UPM process can be found in the previous studies [20, 21]. The raw material used in the micro-UPM process is UHMWPE (Z1700, SAMSUNG). The raw material has the following characteristics: average molecular weight of 3.5 × 10^6 g·mol^{-1}, and average particle size of approximately 150 μm.

Four types of micro-cylinder array parts (micro-UPM parts A, B, C and D) were moulded with powder preheated temperatures 28, 45, 65 and 85 °C respectively, using the PCB micro-cavity inserts shown in figure 1(a), the micro-UPM process parameters of which are as following: ultrasonic duration time of 3.5 s, ultrasonic compression pressure of 40.0 MPa, and holding time of 5.0 s. Two types of micro-cylinder array parts (micro-UPM parts E and F) were moulded with powder preheated temperatures 28 and 85 °C respectively, using the PCB micro-cavity inserts shown in figure 1(b), the micro-UPM process parameters of which are as following: ultrasonic duration time of 3.0 s, ultrasonic compression pressure of 32.0 MPa, and holding time of 5.0 s. The heating time in both cases is 5 min. The micro-cylinder array parts eventually fabricated are shown in figures 1(c) and (d). Subsequently, the micro-cylinder array parts with their corresponding PCB micro-inserts are cold inlaid as a whole, and then the micro-cylinders are polished to their maximum diameters, as shown in figures 1(e) and (f). Finally, the local elastic moduli of the polished micro-cylinders are measured using an *in situ* nano-mechanical testing instrument (TI 950, HYSITRON).

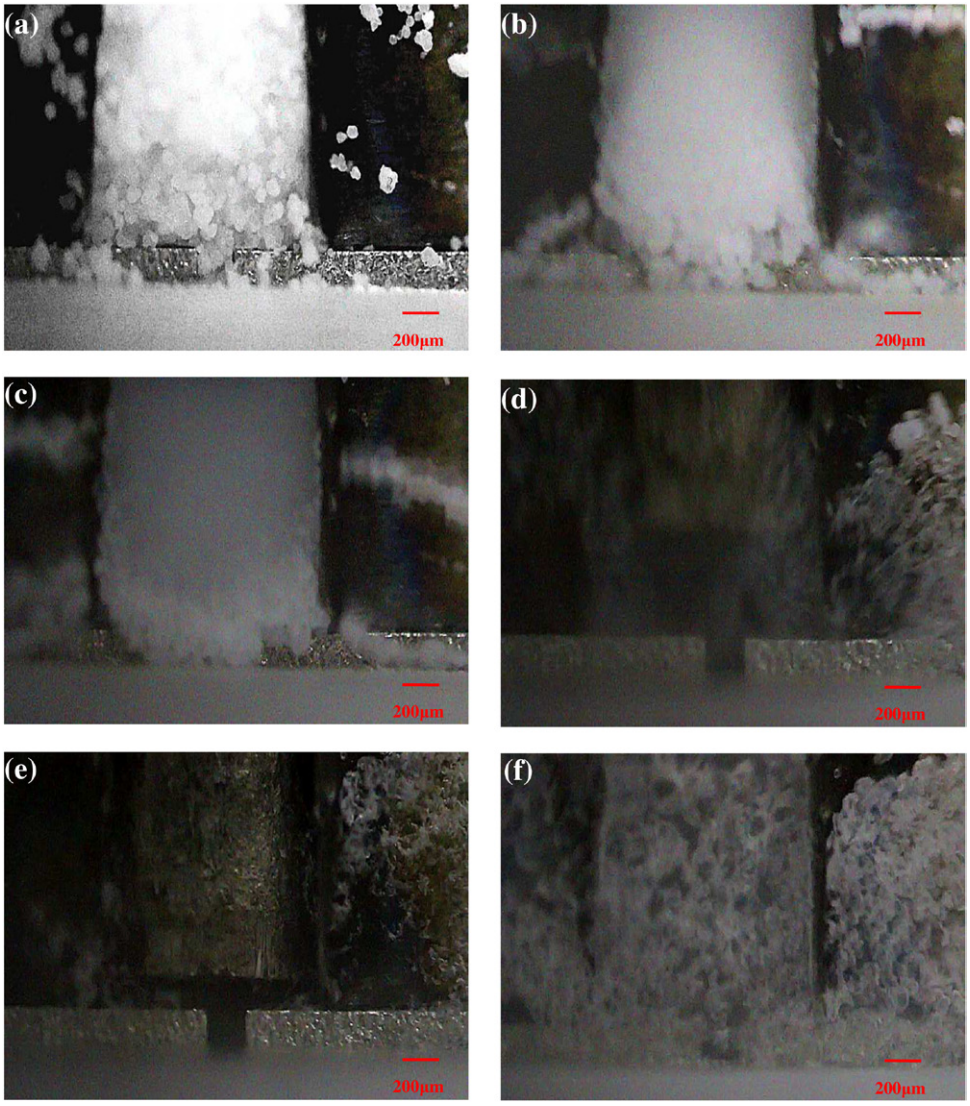

Figure 2. Full-process video of micro-UPM: (a) filling UHMWPE powder; (b) compacting UHMWPE powder; (c) starting ultrasonic vibration; (d) ultrasonic sonotrode goes down; (e) melt fills the entire micro-cavity and (f) holding and cooling times.

3. Results and discussion

3.1. Full-process dynamic ultrasonic plasticisation process and temperature curves

The full-process dynamic ultrasonic plasticisation process (as shown in figure 2) was recorded through quartz glass using a digital single lens reflex camera (EOS 70D, CANON) with a macro lens (MP-E, CANON). As shown in figure 2(a), when the powder particles were first filled in the barrel hole and the micro-cavity, they appeared loose with large interparticle voids. When the ultrasonic sonotrode was used to compact the powders repeatedly at a compression pressure of more than 32.0 MPa, the voids gradually decreased, whereas the interparticle contact area increased, as shown in figure 2(b). With increasing compaction times and compression pressure, the distribution of interparticle voids and the contact area tended to remain constant when the billet density was approximately 0.826 g·cm^{-3}. After the powder particles were repeatedly compacted, the proper ultrasonic plasticisation process parameters were set. The moment the ultrasonic vibration started, high-frequency (20 kHz) friction and compressive deformation among the powder particles occurred. The particles in the barrel hole and the micro-cavity were completely plasticised in a very short time (less than 0.5 s), and they formed a transparent melt pool. The micro-UPM heating mechanisms are similar to ultrasonic welding. According to the previous studies [21] and [23], as a semi-crystalline polymer, the melting temperature of melting-crystallized UHMWPE and the nascent UHMWPE is approximately 135 °C and 142 °C respectively. The crystallinity of Z1700 UHMWPE powder produced by Samsung is 71.3%. As was mentioned in a previous study [22], melting temperature should be taken into consideration to calculate the temperature increasing rate when interfacial friction heating effect dominates.

A temperature measurement module, which was composed of *K*-type thermocouples (TC-TT-K-36-36, OMEGA) and a data acquisition card (USB 9213, NI), was built to record the temperature curves at the bottom and the edge of micro-polymer parts during the micro-UPM process. The layout of the *K*-type thermocouples is shown in figure 3. From

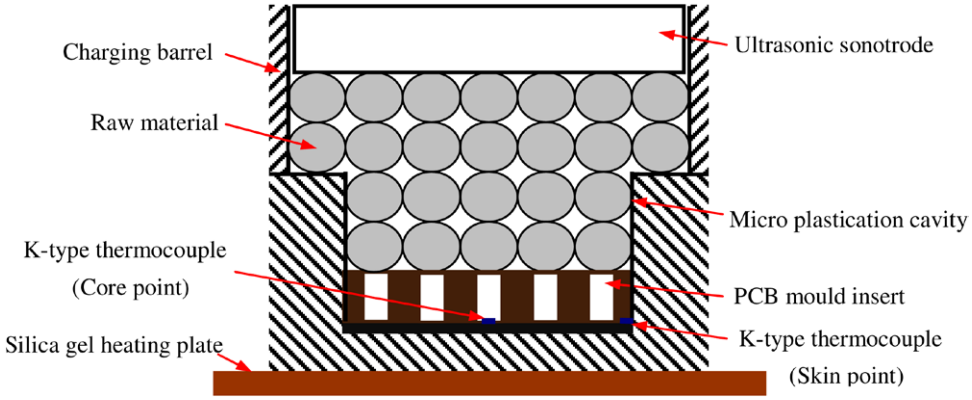

Figure 3. Layout of *K*-type thermocouples.

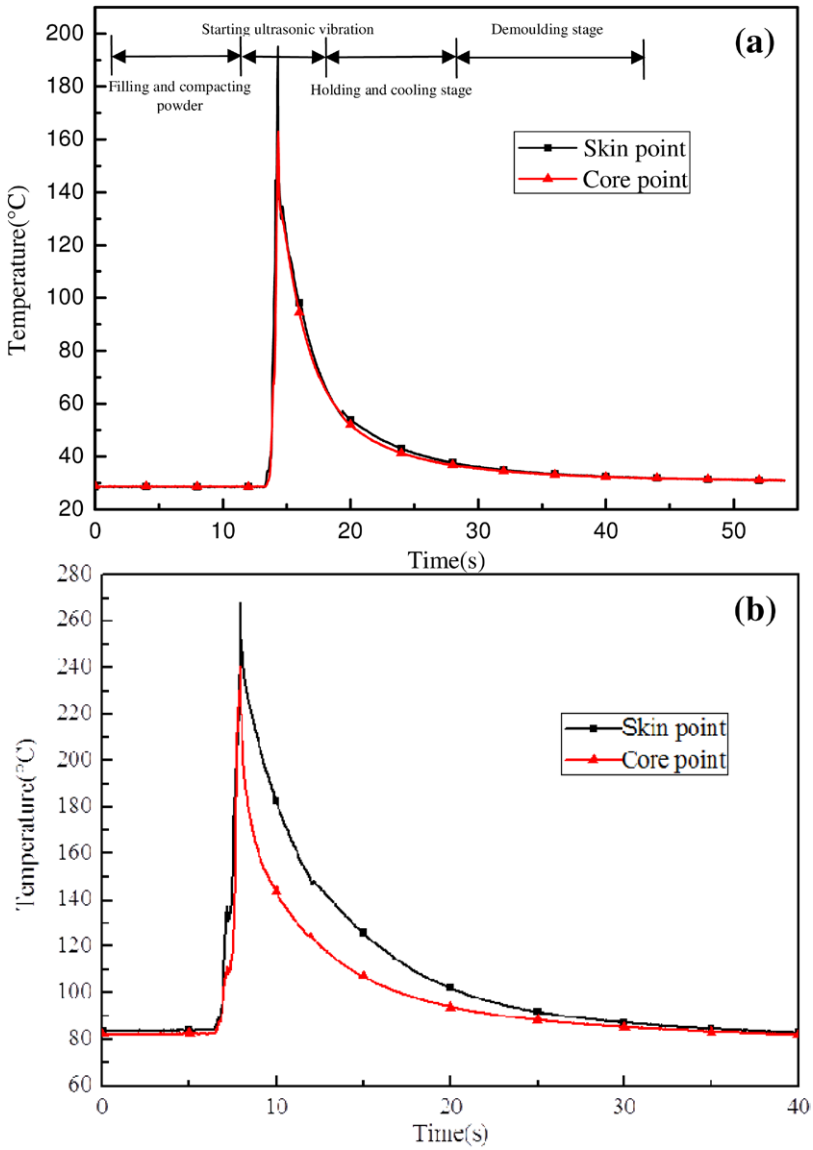

Figure 4. The temperature curves of the core and skin points at the bottom of the micro-UPM parts: (a) micro-UPM part A with powder preheated temperatures 28 °C and (b) micro-UPM part D with powder preheated temperatures 85 °C.

the temperature curve of the skin point at the bottom of the micro-UPM part A shown in figure 4(a), when UHMWPE was transformed into the melting state from room temperature 28 °C to 142 °C, it took 1.22 s, and the temperature increasing rate reached 93 °C·$\mathbf{s}^{-1}$ when interfacial friction heating effect dominated. However, when the temperature increased from 142 °C to 188 °C, it took only 0.14 s. The temperature increasing rate reached as high as 329 °C·$\mathbf{s}^{-1}$, when the

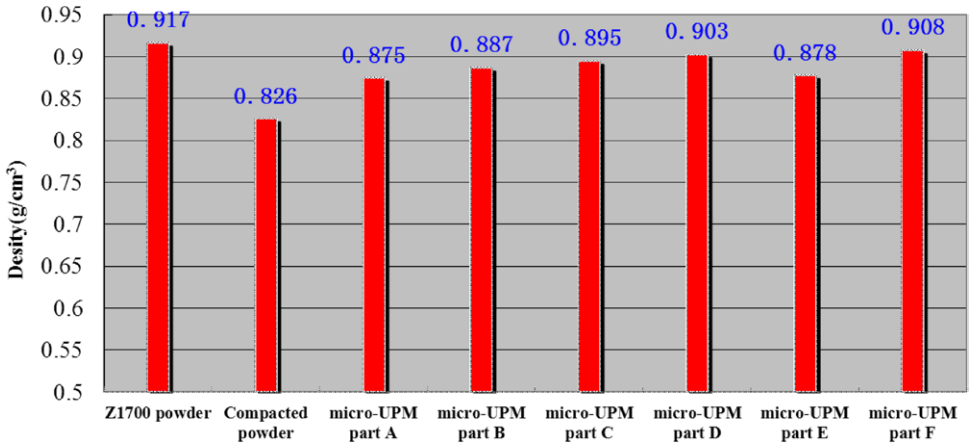

Figure 5. Densities of the raw powder, billets, and micro-UPM parts.

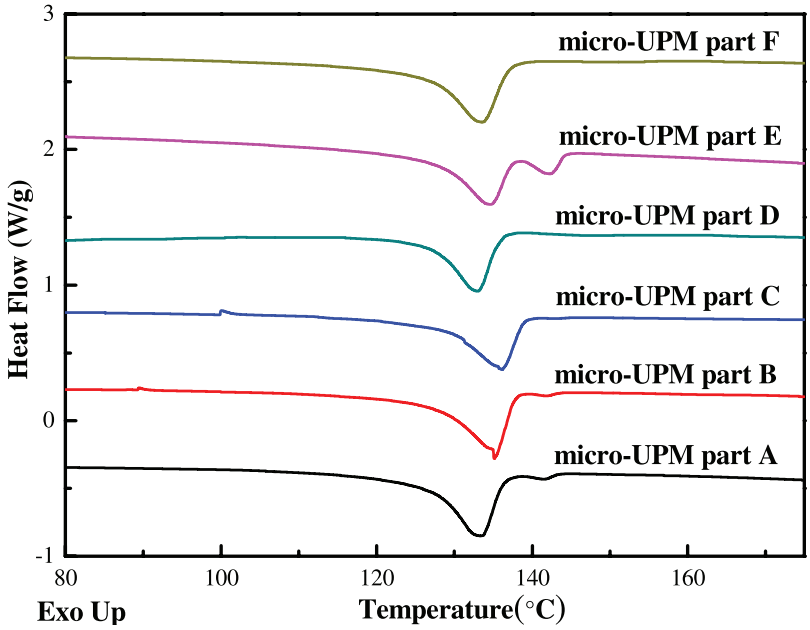

Figure 6. DSC curves of the micro-UPM cylinder array parts.

viscoelastic heating effect dominated, which was about three times the temperature increasing rate when the interfacial friction heating effect dominated. Figure 4(b) is the temperature curves of the core and skin points at the bottom of micro-UPM part D when UHMWPE powder was preheated to 85 °C during the micro-UPM process.

As the ultrasonic sonotrode went down to the bottom of the barrel hole, the transparent polymer melt was continuously forced into the micro-cavity, whereas the extra melt rapidly overflowed upwards along the sonotrode and barrel hole wall. However, some bubbles were found in the melt, as shown in figures 2(c)–(e). When the ultrasonic vibration ended and the holding time began, the melt crystallised at the cooling stage, thereby forming micro-UPM parts and a flash on the top of the barrel. The sonotrode was also wrapped with porous polymer plastics, as shown in figure 2(f).

Following crystallisation, the micro-UPM parts were extracted from the apparatus, and then overflow and flash were removed. After the micro-parts were weighed with a precision electronic balance (FA2104J with an accuracy of 0.1 mg) and their volumes in pure ethanol (0.80 g·ml^{-1}) were measured, the density of the micro-UPM parts could be calculated. Figure 5 shows the average densities of the raw material powder, billet (compacted powders), and five micro-UPM UHMWPE samples from each group with a measurement error of less than 2%. It can be found that the densities of the micro-polymer parts are improved if the raw material powder is preheated. As a result, it can be concluded that preheating powder for some time can significantly improve the quality of ultrasonic plasticisation and decrease the micro-pores of the micro-UPM parts.

Ten samples from each type of micro-cylinder array polymer parts are selected randomly, and the diameter, height, and the cylindrical surface roughness are measured using a scanning electron microscope (S-3400N, HITACHI) and a surface profiler. The

arithmetic mean diameters of the micro-UPM parts D and F are approximately 152.8 and 205.5 μm, and the standard deviations are approximately 2.7 and 2.4, respectively. The arithmetic mean heights of parts D and F are approximately 180.9 and 181.7 μm, and the standard deviations are approximately 1.4 and 1.2, respectively. The arithmetic means of the cylindrical surface roughness of parts D and F are 4.9 and 4.5 μm, respectively, and the standard deviations are both approximately 0.2. When the UHMWPE powder particles with an average diameter of 150 μm (range: 80 ~ 200 μm) fill the micro-cavity, only some of them can be pre-filled into the micro-hole. When heated to 85 °C, the powder particles melt immediately after ultrasonic plasticisation begins, and then they fill the micro-hole under the pressure of ultrasonic sonotrode. Compared with the filling conditions in traditional injection moulding, those of UHMWPE are considerably modified; however, the size effect still exists. As a result, the average diameter of the micro-cylinder polymer parts is 10.0 μm smaller than that of the micro-hole, whereas the roughness of the cylindrical surface is greater than that of the hole wall. The heights are almost the same.

3.2. Two-phase structure of the micro-UPM parts analysed using DSC

The melting temperature (T_m) of the micro-UPM cylinder array parts is measured using DSC (Q200, TA). The melting enthalpy ΔH is calculated and fitted using TA Universal Analysis 2000. Generally, the crystallinity (X_C) of the UHMWPE polymer may be obtained via dividing the melt enthalpy (ΔH) by the 100% crystal of the standard melt enthalpy (ΔH^*). The UHMWPE standard melt enthalpy is 291.0 J·g^{-1} [21, 23].

As mentioned in previous studies [20, 24], T_m of the nascent UHMWPE is approximately 142 °C, and T_m of the melt-recrystallised UHMWPE is 135 °C. In figure 6, the DSC curves of the micro-UPM cylinder parts with two melting peaks can be seen as a bi-phased material of nascent and melt-recrystallised UHMWPE; the T_m of micro-UPM parts A and E are 135 °C and 143 °C, respectively, which are consistent with the two T_m mentioned in the previous studies [20, 24]. The value of X_C of micro-UPM parts A and E are 58.4% and 57.0%, respectively. The micro-UPM cylinder polymer part consists of both nascent and melt-recrystallised phases because the base of the micro-UPM part is relatively large and ultrasonic power is inadequate, leading to incomplete plasticisation. Therefore, if powder particles are not preheated, the micro-UPM cylinder parts are normally in a two-phase structure.

When the temperature ranges from 45 °C to 85 °C, it can be seen from figure 6 that the area of the nascent state melting peak decreases while the area of the melt-recrystallised melting peak increases. When the temperature reaches 85 °C, only a single melt-recrystallised melting peak exists, and the melting temperature is approximately 134 °C, as shown on the DSC curves. The X_C of micro-UPM parts D and F are close, 54.7% and 55.2% respectively.

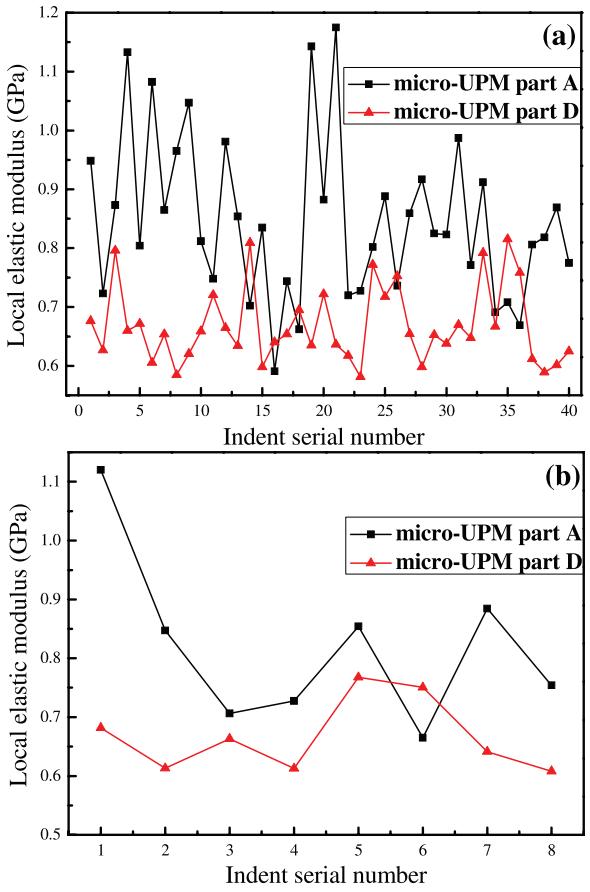

Figure 7. Local elastic modulus of the micro-UPM part: (a) base region and (b) micro-cylinder region.

3.3. Two-phase structure of the micro-UPM parts analysed using nanoindentation tests

According to the previous studies [25–27], the UHMWPE polymer parts moulded by high-velocity compaction (HVC) consist of both nascent and melt-recrystallised phases; nascent UHMWPE is of high X_C, so its rigidity is better than that of melt-recrystallised UHMWPE. The extrapolation indicates that the estimated elastic modulus of the nascent UHMWPE is approximately twice that of the melt-recrystallised UHMWPE [21, 26].

The nanoindentation tests are conducted on the surfaces of the micro-UPM UHMWPE samples using a standard Berkovich tip. The selected samples are the micro-cylinder and base regions of the micro-UPM parts A and D with an average diameter of 150 μm. On the base region, 40 indentations numbered from 1 to 40 with a 20 μm interval formed a 780 μm-long segment, which is much longer than the average UHMWPE particle size of 150 μm (the size distribution of Z1700 powder particles ranged from 80 μm to 200 μm). Regarding the micro-cylinder region, 8 indentations numbered from 1 to 8 in the axial direction on the micro-cylinder slices shown in figures 1(e) and (f) are spaced at a 20 μm interval to form a 140 μm-long segment. As concluded in the previous study [20], the local elastic modulus (E_r) of the micro-UPM UHMWPE part in the nanoindentation tests ranged from 0.7 ~ 1.1 GPa, with a variation range of 0.4 GPa.

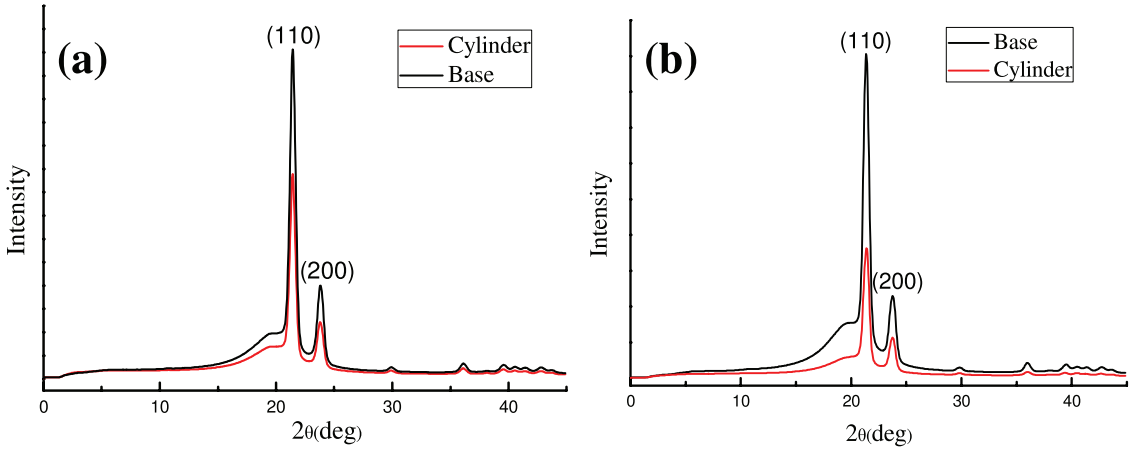

Figure 8. X-ray diffraction patterns of the micro-UPM parts: (a) micro-UPM part D and (b) micro-UPM part F.

Table 1. Single-crystal XRD test results of micro-UPM cylinder array parts.

Sample	Test region	Main crystal surface	2θ (°)	Interplanar spacing (Å)	Crystallinity X_C
micro-UPM part **D** (0.15 mm)	Micro-cylinder	110	21.4	4.14	59.9%
		200	23.8	3.73	
	Base	110	21.4	4.14	63.2%
		200	23.8	3.72	
micro-UPM part **F** (0.20 mm)	Micro-cylinder	110	21.3	4.15	61.7%
		200	23.8	3.73	
	Base	110	21.4	4.15	64.5%
		200	23.8	3.74	

The area of higher E_r corresponded to the nascent UHMWPE, whereas the lower E_r corresponded to the melt-recrystallised UHMWPE.

Figure 7 is the distribution ranges of E_r of the base and cylinder region of micro-UPM parts A and D. Figure 7 shows that, except for a few indentations, the range of E_r of the base and micro-cylinder region of micro-UPM part A is from 0.7 GPa to 1.2 GPa, close to the distribution ranges of E_r provided by the previous study [21], but much less than the HVC test results in another study [26]. Therefore, it can be concluded that the micro-UPM cylinder part A consists of nascent and melt-recrystallised phases, consistent with the DSC test results in section 3.2.

For micro-UPM part D, except for a few indents, the E_r of the base and micro-cylinder region both range from 0.6 GPa to 0.8 GPa, close to the lower limit of E_r in the previous study [21]. Therefore, it can be concluded that micro-UPM part D consists of the melt-recrystallised phase, consistent with the DSC test results in section 3.2.

3.4. The research of phase structure development by single-crystal XRD

Figure 8 shows the one-dimension diffraction patterns of the base and micro-cylinder region of micro-UPM parts D and F obtained using single-crystal XRD (RAPID, RIGAKU). The micro-cylinder region can be tested by x-rays penetrating from the wall surface. The base region was tested by x-rays penetrating from the top surface. From the X_C calculated by Jade 6.0 shown in table 1, the X_C of the base region is higher than that of the micro-cylinder region; the grain size of the (1 1 0) crystal surface is larger than that of the (2 0 0) crystal surface.

4. Conclusion

In this study, two types of micro-cylinder array parts were moulded using preheated UHMWPE powder via the micro-UPM process and the conclusions are as follows:

(1) PCB micro-cavity inserts with micro-hole arrays were fabricated by high-speed mechanical drilling and two types of micro-cylinder polymer parts of diameter 0.15 mm and 0.20 mm were moulded through micro-UPM. Results of the cold inlaid experiment reveal that the average diameter of the micro-cylinder polymer parts is 10.0 μm smaller than that of the micro-hole.

(2) A visualized ultrasonic plasticisation moulding experiment platform with a temperature measurement module was built to record the temperature curves at the bottom of the micro-UPM part, and then the temperature increasing rate was calculated. The result revealed that when viscoelastic heating dominated, the temperature increasing rate was about three times the rate when interfacial friction heating effect dominated. A digital single lens reflex camera with a macro-lens was used to record the full-process dynamic ultrasonic plasticisation, including compacting UHMWPE powder, starting ultrasonic vibration, filling the entire micro-cavity with the polymer melt and cooling the micro-UPM part during the holding stage.

(3) When UHMWPE powder was preheated from room temperature 28 °C to 85 °C, the densities of the micro-polymer parts was found to be increased. Preheating powder for some time can not only significantly improve the quality but decrease the micropores and the size effect of micro-UPM parts.

(4) According to the DSC and nanoindentation test results, if the UHMWPE powder is not preheated, then the micro-cylinder array polymer parts generally consisted of nascent and melt-recrystallised phases as a whole. However, when UHMWPE powder was preheated from room temperature of 28 °C to 85 °C, the two-phase structure gradually developed into a single melt-recrystallised phase. According to the single-crystal XRD test result, the value of X_C of the base region of the micro-UPM polymer part is higher than that of the micro-cylinder region, whereas the grain size of the (1 1 0) crystal surface is higher than that of the (2 0 0) crystal surface.

Acknowledgments

This work is supported by the National Natural Science Foundation of China (No. 51575360, 51175348, 51405306 and 51501116), and the Research and Development Foundation of Science and Technology of Shenzhen (No. JCYJ20150525092941026 and JCYJ20140418095735629). The authors are grateful to Shenzhen Jinzhou Precision Technology Corp., for their generous offer of experimental equipment and to colleagues for their essential contribution to the work.

References

[1] Chang C Y, Yang S Y, Huang L S and Chang J H 2006 Fabrication of plastic microlens array using gas-assisted micro-hot-embossing with a silicon mold *Infrared Phys. Tech.* **48** 163–73

[2] Jo S B, Lee M W, Park S G, Suh J K and Beom-Hoan O 2004 Fabrication and surface treatment of silicon mold for polymer microarray *Surf. Coat. Tech.* **188** 452–8

[3] Takahata K and Gianchandani Y B 2002 Batch mode micro-electro-discharge machining *J. Microelectromech. Syst.* **11** 102–10

[4] Kurita T, Chikamori K, Kubota S and Hattori M 2006 A study of 3D shape machining with an ECμM system *Int. J. Mach. Tools Manuf.* **46** 1311–18

[5] Lu Z and Zhang K F 2009 Morphology and mechanical properties of polypropylene micro-arrays by micro-injection molding *Int. J. Adv. Manuf. Tech.* **40** 490–6

[6] Cherng Y S and Su G D J 2014 Fabrication of polydimethylsiloxane microlens array on spherical surface using multi-replication process *J. Micromech. Microeng.* **24** 015016

[7] Liu Y S, Zhang P, Deng Y B, Hao P, Fan J H, Chi M B and Wu Y H 2014 Polymeric microlens array fabricated with PDMS mold-based hot embossing *J. Micromech. Microeng.* **24** 095028

[8] Fu L Y and Yang F 2008 A solution for PCB drilling with strict requirement on hole wall quality *Circuit World* **34** 8–11

[9] Fu L Y, Li X G and Guo Q 2010 Development of a micro drill bit with a high aspect ratio *Circuit World* **36** 30–4

[10] Liang X, Li B, Wu X Y, Shi H Y, Zeng K and Wang Y T 2013 Micro UHMW-PE column array molded by the utilization of PCB as mold insert *Circuit World* **39** 95–101

[11] Ma J, Huo L S, Zhao D Q and Wang W H 2013 Micro mold filling kinetics of metallic glasses in supercooled liquid state *J. Appl. Phys.* **113** 104505

[12] Ma J, Zhang X and Wang W H 2012 Metallic glass mold insert for hot embossing of polymers *J. Appl. Phys.* **112** 024506

[13] Zhang X, Ma J, Fang G, Sun B L, Li J F and Li Q 2014 Polymer micro molding with bulk metallic glass mold *Microsyst. Technol.* **21** 1453–57

[14] Fairbanks H V 1974 Applying ultrasonics to the moulding of plastic powders *Ultrasonics* **12** 22–4

[15] Paul D W and Crawford R J 1981 Ultrasonic moulding of plastic powders *Ultrasonics* **19** 23–7

[16] Michaeli W, Kamps T and Hopmann C 2011 Manufacturing of polymer micro parts by ultrasonic plasticization and direct injection *Microsyst. Technol.* **17** 243–9

[17] Sacristan M, Planta X, Morell M and Puiggalí J 2014 Effects of ultrasonic vibration on the micro-molding processing of polylactide *Ultrason. Sonochem.* **21** 376–86

[18] Planellas M, Sacristan M, Rey L, Olmo C, Aymamí J, Casas M T, del Valle L J, Franco L and Puiggalí J 2014 Micro-molding with ultrasonic vibration energy: New method to disperse nanoclays in polymer matrices *Ultrason. Sonochem.* **21** 1557–69

[19] Wu S Y, Wu X Y, Xu B, Cheng R, Luo F and Ruan S C 2014 A micro-ultrasonic powder moulding method to fabricate Sn–Bi alloy micro parts *J. Mater. Process. Tech.* **214** 2668–75

[20] Zeng K, Wu X Y, Liang X, Xu B, Wang Y T, Chen X Q, Cheng R and Luo F 2013 Process and properties of micro-ultrasonic powder molding with polypropylene *Int. J. Adv. Manuf. Tech.* **70** 515–22

[21] Liang X, Wu X Y, Zeng K, Xu B, Wu S Y, Zhao H, Li B and Ruan S C 2014 Micro ultrasonic powder molding for semi-crystalline polymers *J. Micromech. Microeng.* **24** 045014

[22] Zhang Z, Wang X D, Luo Y, Zhang Z G and Wang L D 2009 Study on heating process of ultrasonic welding for thermoplastics *J. Thermoplast. Compos.* **23** 647–64

[23] Reggiani M, Tinti A, Taddei P, Visentin M, Stea S, De Clerico M and Fagnano C 2006 Phase transformation in explanted highly crystalline UHMWPE acetabular cups and debris after *in vivo* wear *J. Mol. Struct.* **785** 98–105

[24] Jauffrès D, Lame O, Vigier G, Doré F and Chervin C 2007 Mechanical and physical characterization of polyoxymethylene processed by high-velocity compaction *J. Appl. Polym. Sci.* **106** 488–97

[25] Jauffrès D, Lame O, Vigier G and Doré F 2007 Microstructural origin of physical and mechanical properties of ultra high molecular weight polyethylene processed by high velocity compaction *Polymer* **48** 6374–83

[26] Jauffrès D, Lame O, Vigier G and Doré F 2009 Sintering mechanisms involved in high-velocity compaction of nascent semicrystalline polymer powders *Acta Mater.* **57** 2550–9

[27] Labour T, Ferry L, Gauthier C, Hajji P and Vigier G 1999 α- and β-crystalline forms of isotactic polypropylene investigated by nanoindentation *J. Appl. Polym. Sci.* **74** 195–200